NORTHEAST NUCLEAR ENERGY COMPANY

MILLSTONE NUCLEAR POWER STATION, UNIT NO. 2

THERMAL SHIELD DAMAGE RECOVERY PROGRAM

FINAL REPORT

APPENDIX A

EFFECTS OF CORE BARREL BYPASS FLOW ON FUEL ASSEMBLIES

TESTING AND ANALYSES

Docket No. 50-336

MARCH, 1984

A.1 Experimental Investigation of Core Shroud Bypass Flow

EXECUTIVE SUMMARY

This report summarizes an experimental investigation to determine the velocity and breadth of flow leaking through a full-scale model of a structural seam in the core fuel shroud assembly. The test program provides data which can be used to assess the flow-induced vibration of fuel rods adjacent to the shroud assembly. The work was done at this time to support evaluation of potential effects of holes drilled recently in the core barrel of the Millstone 2 Plant to arrest a crack.

Tests were conducted in a full-scale model of a sector of the core barrel/shroud assembly. The full-scale model was used to make direct measurements of the leakage velocity at several values of downcomer-to-core pressure drop specified by Northeast Utilities for these tests. The results show that the leakage velocity is approximately 50% of the velocity of the flow through the crack-arrestor hole for the configuration which was tested. At the specified pressure drop of 25 psi, a velocity of 30 ft/sec was measured over a span of about 2.25 inches through a seam 0.015 inches wide. Further, measurements in the model indicate that the leakage velocity is proportional to the square root of seam width and to the square root of downcomer-to-core pressure drop.

A flow visualization model was used to provide a qualitative assessment of the flow patterns which establish the conditions for this leakage flow. Some data are presented which show that the height of the leakage flow is restricted to a small region of the seam length equivalent to a few diameters of the inlet jet and is bounded by the girth rib at the inlet jet elevation. Pressure measurements were also made in the region between the core barrel and the core shroud. These measurements and observations are used to develop a brief description of the flow phenomena and to support calculations we have performed. A self-consistent description of the velocity distribution throughout the model is presented and compared with theory.

Creare R&D Incorporated carried out this work for Northeast Utilities Service Company under Purchase Order 828493. Tests in the full-scale model were conducted following Quality Assurance procedures meeting the requirements of ANSI N45.2. The Northeast Utilities representative for this work was Frank Mello; the authors were responsible for carrying out the test program.

TABLE OF CONTENTS

LIST OF TABLES

LIST OF FIGURES

1 INTRODUCTION

This report describes an experimental project carried out by Creare R&D Inc. to measure the velocity of flow leaking through a structural seam in a full-scale model of the core fuel shroud assembly. This leaking flow is supplied from the flow through a crack-arresting hole in the core barrel, driven by the downcomer-to-core differential pressure. The leakage flow is of concern because it can impact directly on a fuel rod located at the exit of the seam, possibly causing erosion or vibration-induced damage to the fuel rod.

Test measurements were made at several downcomer-to-core differential pressure values, bracketing the target operating pressure drop of 25 psid specified by Northeast Utilities. The test model was supplied by Northeast Utilities and assembled to have a nominal seam width of 0.015 inch which was specified by Northeast Utilities.

A separate flow visualization model was also constructed to provide additional experimental verification of the extent of the flow leaking through the seam and direct observation of the overall flow patterns.

Section 2 of this report describes the test model, facility and instrumentation used in the tests of the full-scale model. The results of the quality-assured tests carried out in that full-scale model are presented and discussed in Section 3. Section 4 describes the flow visualization model and the flow measurements and observations derived from that model. An interpretation of the observations from the flow visualization studies is given in Section 5. Additional measurements from preliminary tests in the full-scale model are documented in Appendix A. Those measurements show the effect of differential pressure and seam width on the velocity of flow leaking through the seam.

The test program described in Sections 2 and 3 was carried out under Quality Assurance procedures described in the Test Plan and Procedures document (Reference 1).

2 FULL-SCALE MODEL TEST PROGRAM

This section describes the test model and facility used to produce data on the velocity of flow leaking through the seam in the shroud assembly.

2.1 Test Model

The measurements of flow velocity were made in a full-scale mockup of an approximately 30° sector of the fuel shroud assembly. The partially assembled test section is shown in Figure 1. It consists of a steel fabrication which provided a realistic full-scale simulation of the important region between the core barrel and the shroud assembly. The shroud seam is formed at the intersection of two panels which form the central "wedge" of the shroud assembly. All dimensions in the mockup were maintained at nominal full-scale values. The vertical extent of the test section spanned the height of three former plates (girth ribs). The as-built dimensions of the model are shown in Figure 2.

The three girth ribs in the model were fabricated from 1.5 inch thick steel plate with one edge of each rib having a radius of curvature of about 73.7 inch (estimated from measurements of the arc height and length). Steel plates (0.75 inch thick) were welded between the girth ribs, intersecting at right angles, to form a sector of the fuel shroud assembly. In the lower half of the mockup the panels forming the central wedge were fabricated from acrylic plates and were adjustable in order to establish the specified seam width for the tests. Additional support brackets were used near the apex of these wedge panels to stabilize the seam width during tests.

The core barrel was simulated in the model using a 0.375 inch thick steel plate having a radius of curvature which conformed to the shape of the girth ribs. The core barrel plate was bolted to 0.375 inch thick flat bars welded to the girth ribs. These bars provided a fixed clearance gap in the model between the inner surface of the core barrel plate and the girth ribs.

In order to simulate the conditions for flow through the core barrel crack-arresting hole, a 1.125 inch diameter hole was drilled through the core barrel plate and through a 1.25 inch thick steel block attached to the plate. The total hole length was 1.625 inch. The core hole was centered in the plane of the seam with its centerline elevation one-half of the hole diameter below the bottom of the middle former plate. Figure 3 clearly shows the alignment of the hole relative to the former plate.

An inlet flow plenum chamber was attached to the core barrel plate as shown in Figure 4. The plenum chamber provided a relatively stagnant flow situation in the tests and was used to define the downcomer-to-core differential pressure.

2.2 Test Facility

In these experiments the fully-assembled mockup (Figure 5) was placed inside a tank and the plenum was connected to a water supply manifold using the 4 hoses as shown in Figure 6. The test facility is shown in Figure 7. Flow to the model was provided from a supply tank using a centrifugal pump with sufficient head to achieve the desired inlet plenum pressure. The flow rate to

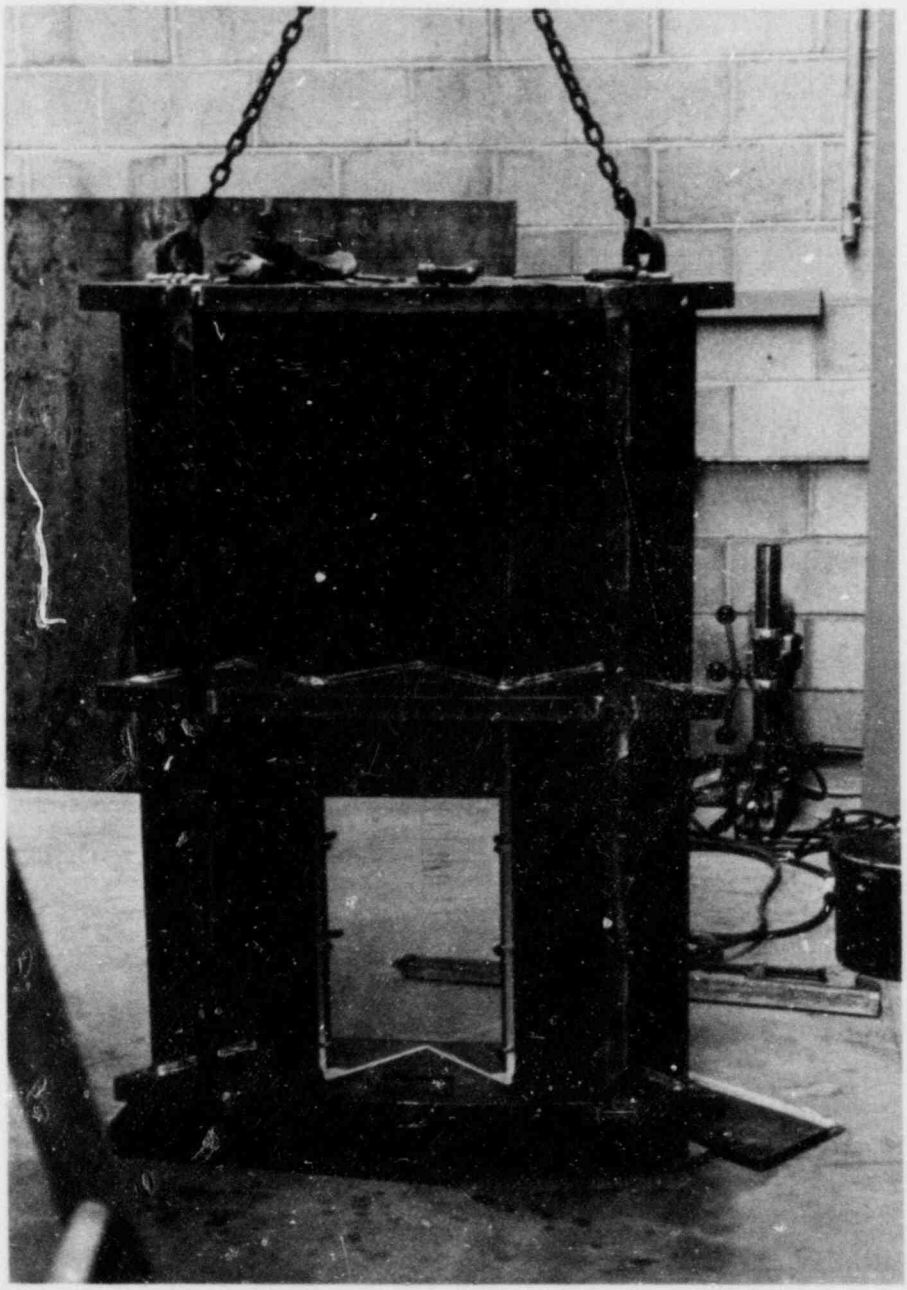

Figure 1. FULL-SCALE TEST MODEL
(Partially Assembled)

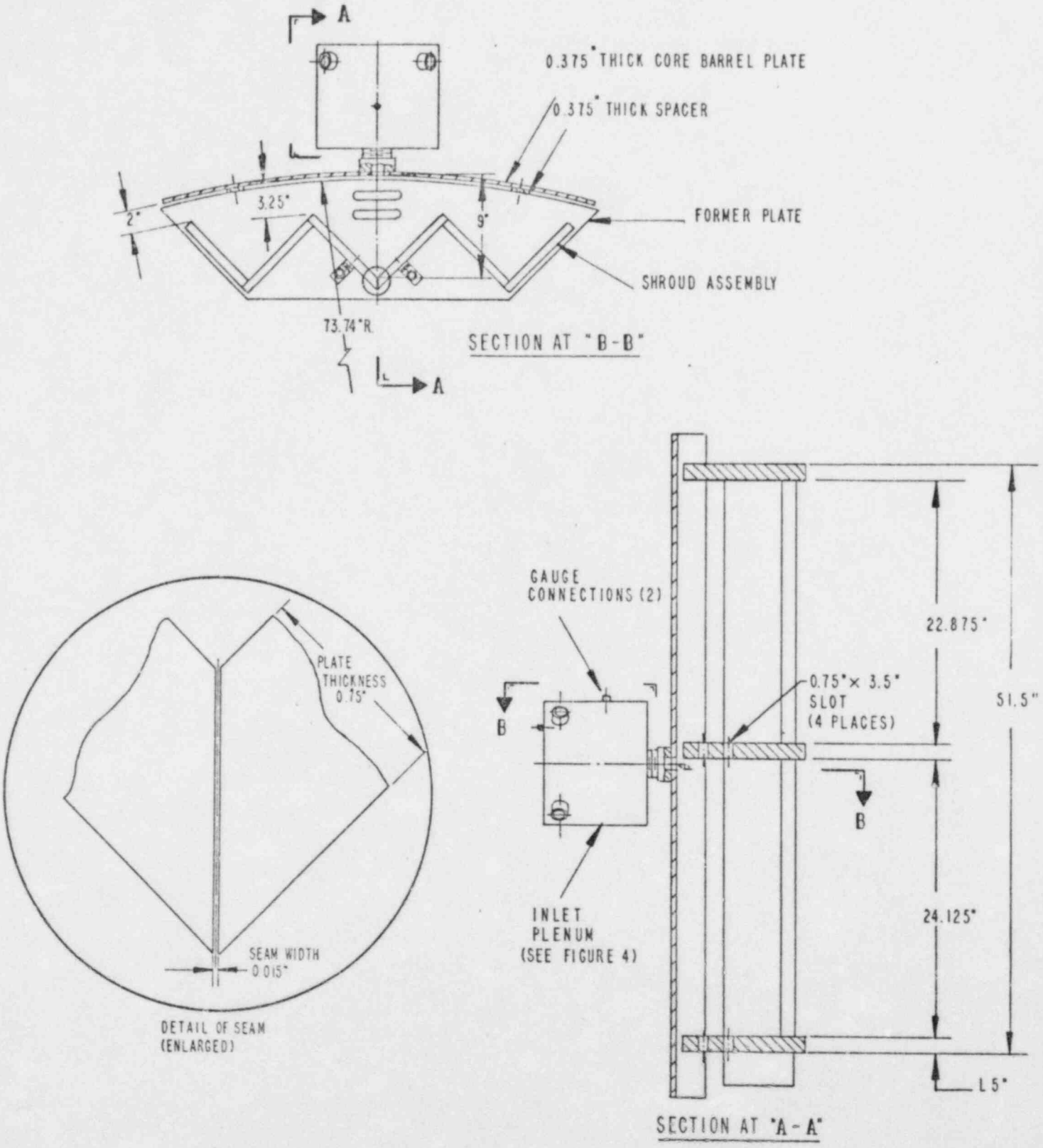

Figure 2. TEST MODEL DIMENSIONS

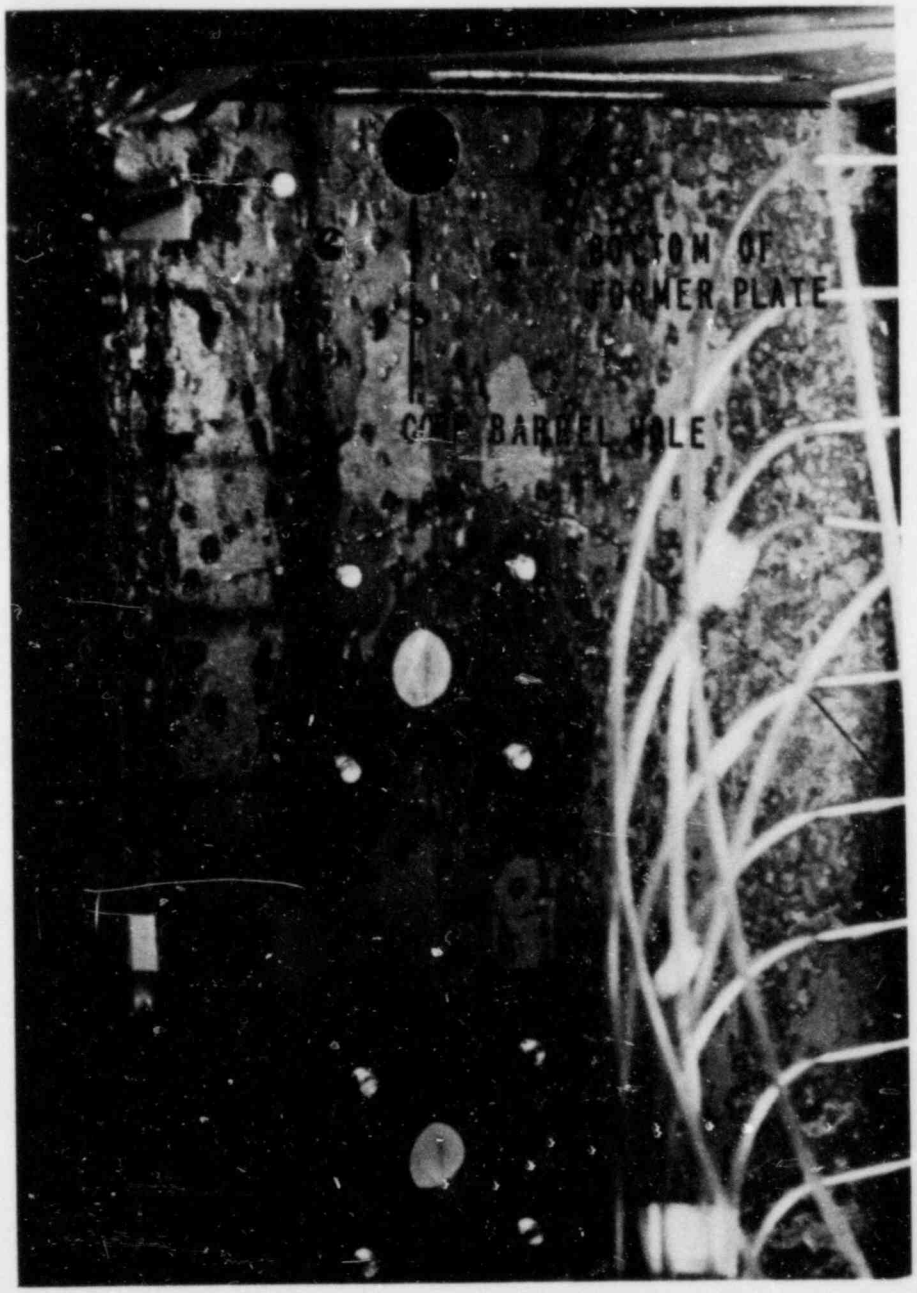

Figure 3. CORE BARREL HOLE IN RELATION TO FORMER PLATE
(Viewed from "Core")

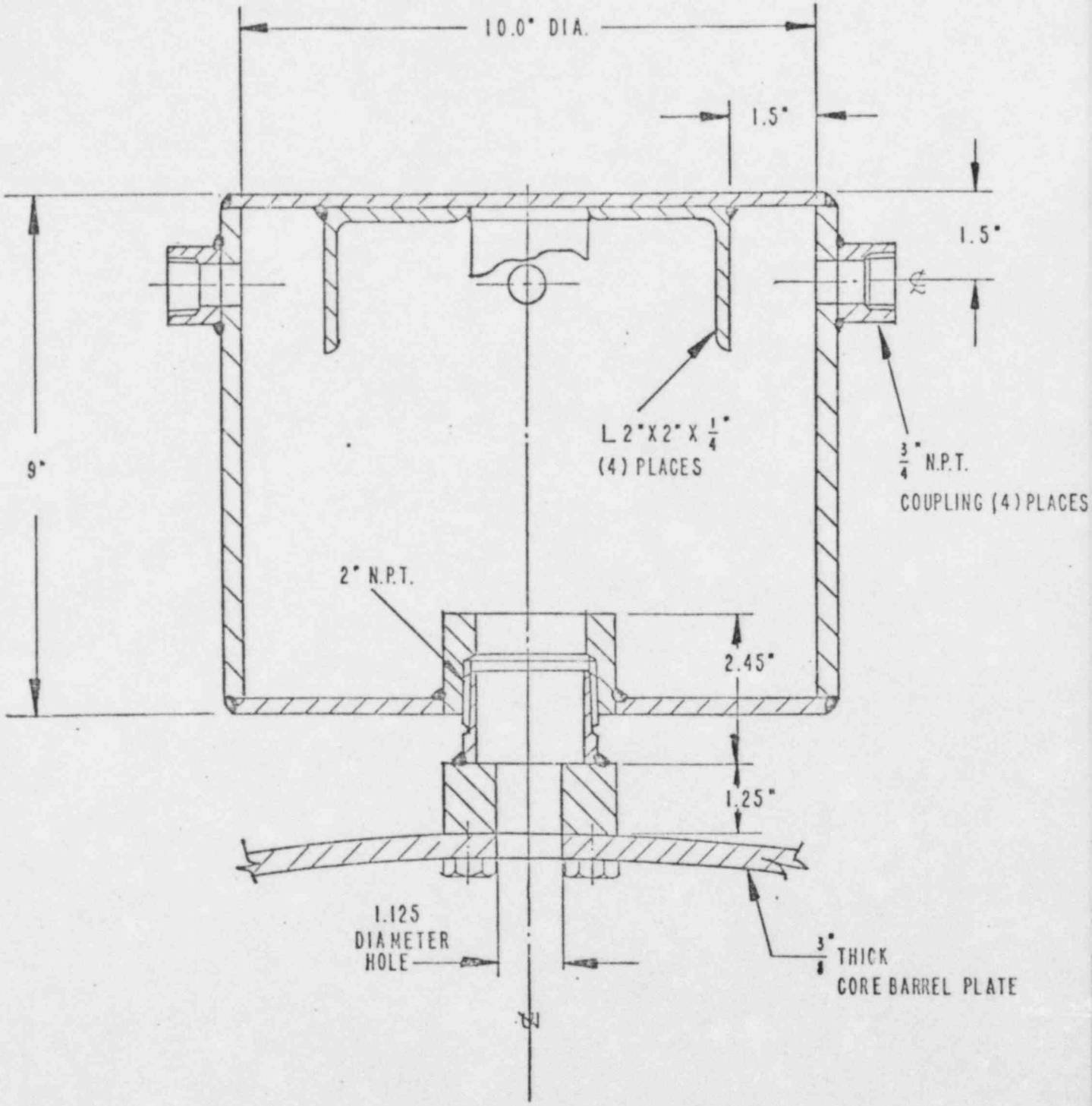

Figure 4. PLENUM CHAMBER DETAILS

Figure 5. ASSEMBLED TEST MODEL

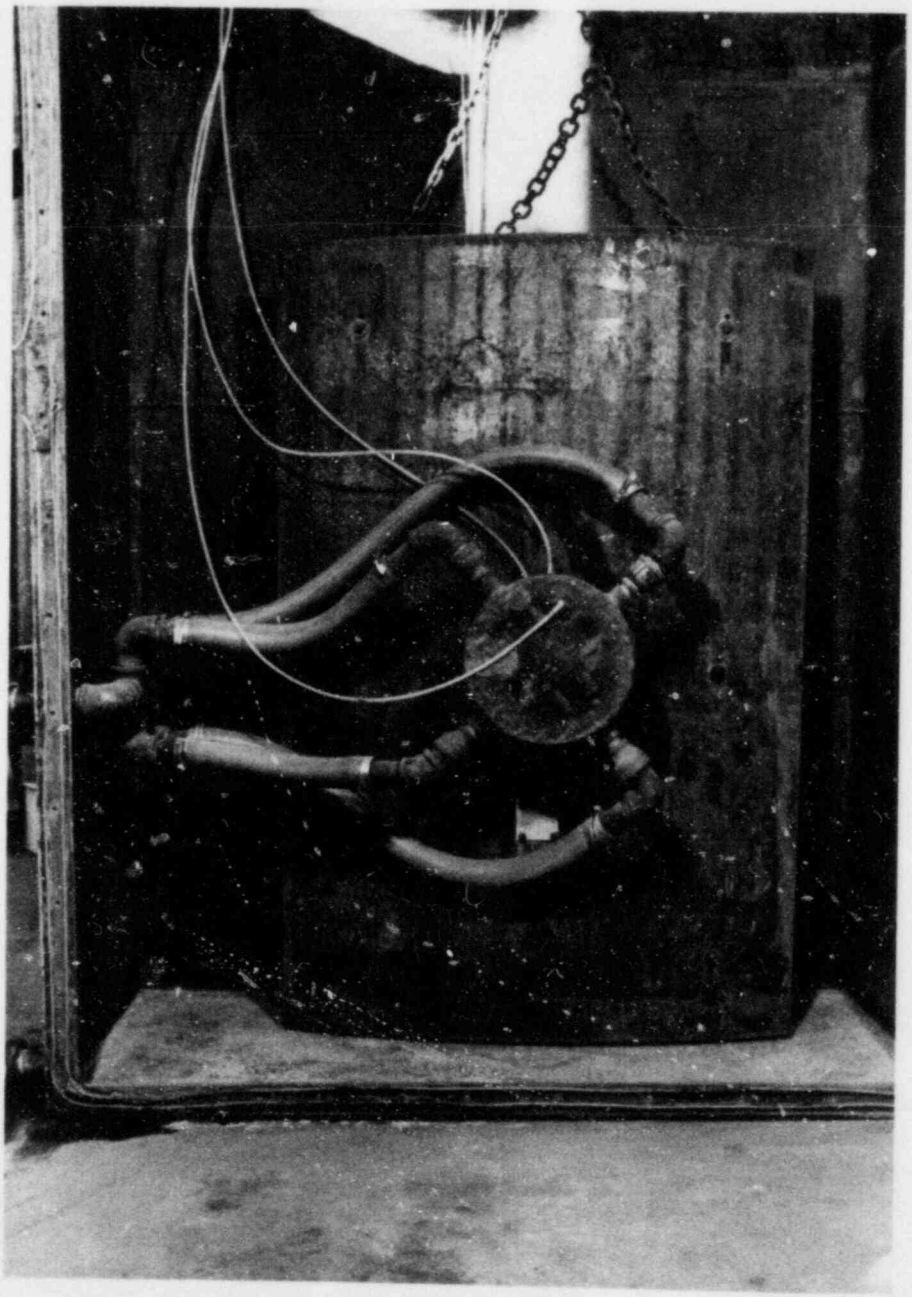

Figure 6. ASSEMBLED TEST MODEL IN TEST FACILITY

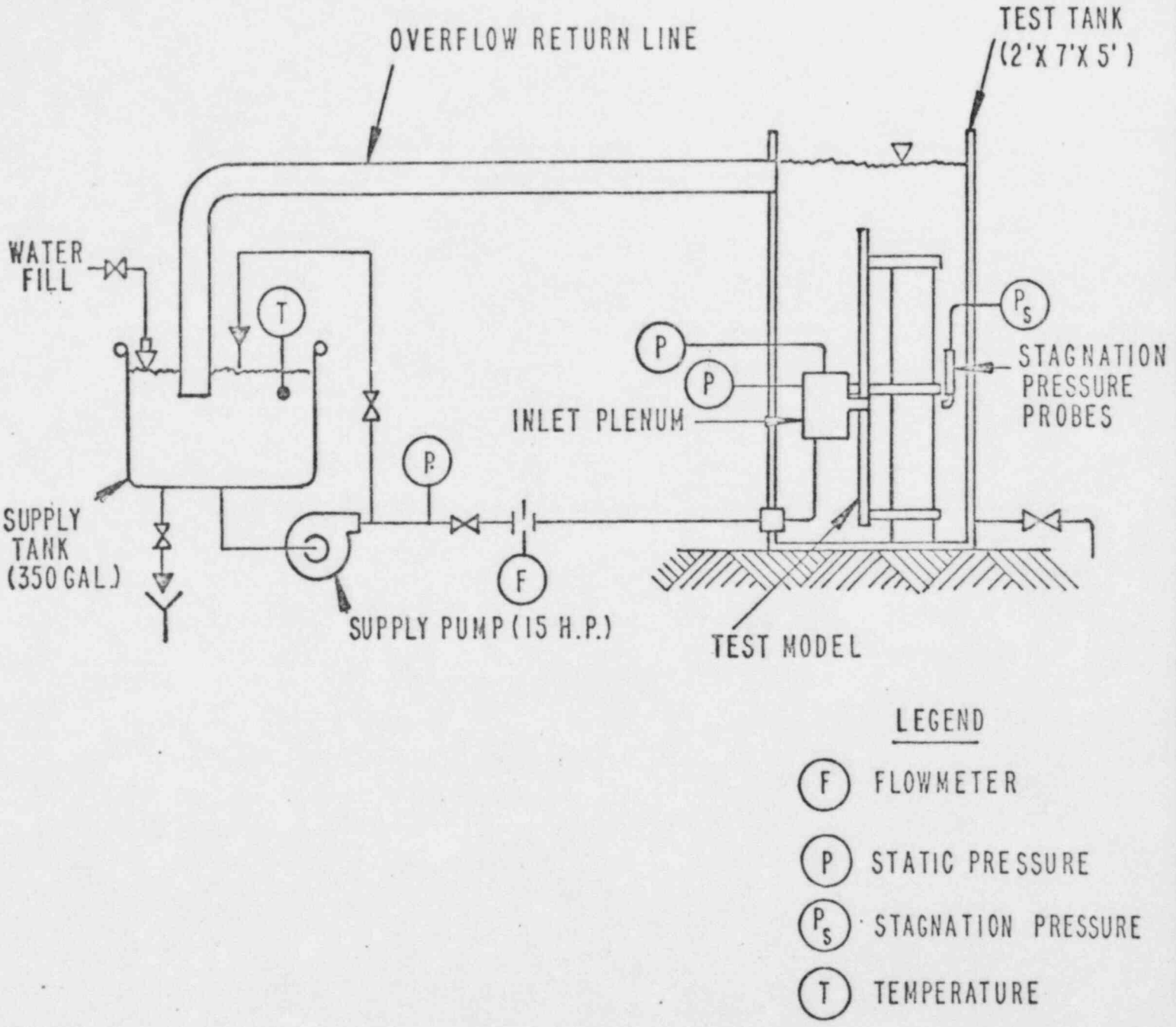

Figure 7. TEST FACILITY SCHEMATIC

the model was regulated using bypass and flow control valves to establish the target inlet plenum pressure. The water leaving the model (through the shroud seam and through the clearance gaps between the core barrel and the shroud assembly) was returned to the supply tank through the overflow line near the top of the test tank. In the tests the model was fully submerged in the tank and the static (no flow) elevation of the water was 26.4 inch above the upper former plate (44.63 inch above the centerline elevation of the core hole). With an inlet plenum pressure of 25 psid, the flow rate into the model was about 155 gallon/minute. (For that flow rate, the water level in the tank head was increased 4.5 inch; this minor change is accounted for in reducing the test data.)

2.3 Test Measurements

The principal measurement of interest in these experiments was the velocity of the flow leaking through the seam in the shroud assembly. Stagnation probes were installed at the exit of the seam to measure the total pressure of the leaking flow, as shown in Figure 8.

These stagnation probes measure the flow velocity according to the relationship:

$$\Delta P = K \frac{\rho V^2}{2g_c} \qquad (1)$$

where ΔP is the difference between the total pressure measured with flow and the pressure measured with no flow (lbf/ft^2)

K is the probe pressure coefficient

ρ is the fluid density (lbm/ft^3)

V is the fluid velocity (ft/s)

g_c is the gravitational proportionality constant ($32.174\ lbm\ ft/lb_f\ s^2$)

For the stagnation pressure probe design used in this test program, the pressure coefficient K is taken to be unity (Reference 2). Thus, the velocity is calculated from:

$$V = \left(\frac{2g_c \Delta P}{\rho} \right)^{1/2} \qquad (2)$$

The probes were fabricated from 0.020 inch diameter stainless steel tubing having an inner diameter of 0.010 inch. The probe tips were placed approximately 0.020 inch from the exit plane of the seam and were aligned to be on the centerline of and perpendicular to the seam. Seven probes were used to define the velocity profile in the region of the maximum expected leak flow velocities and extending approximately 3.25 inch below the middle former plate.

The probes were connected to a single pressure transducer using water-filled lines and isolation valves. During the tests the valves were used

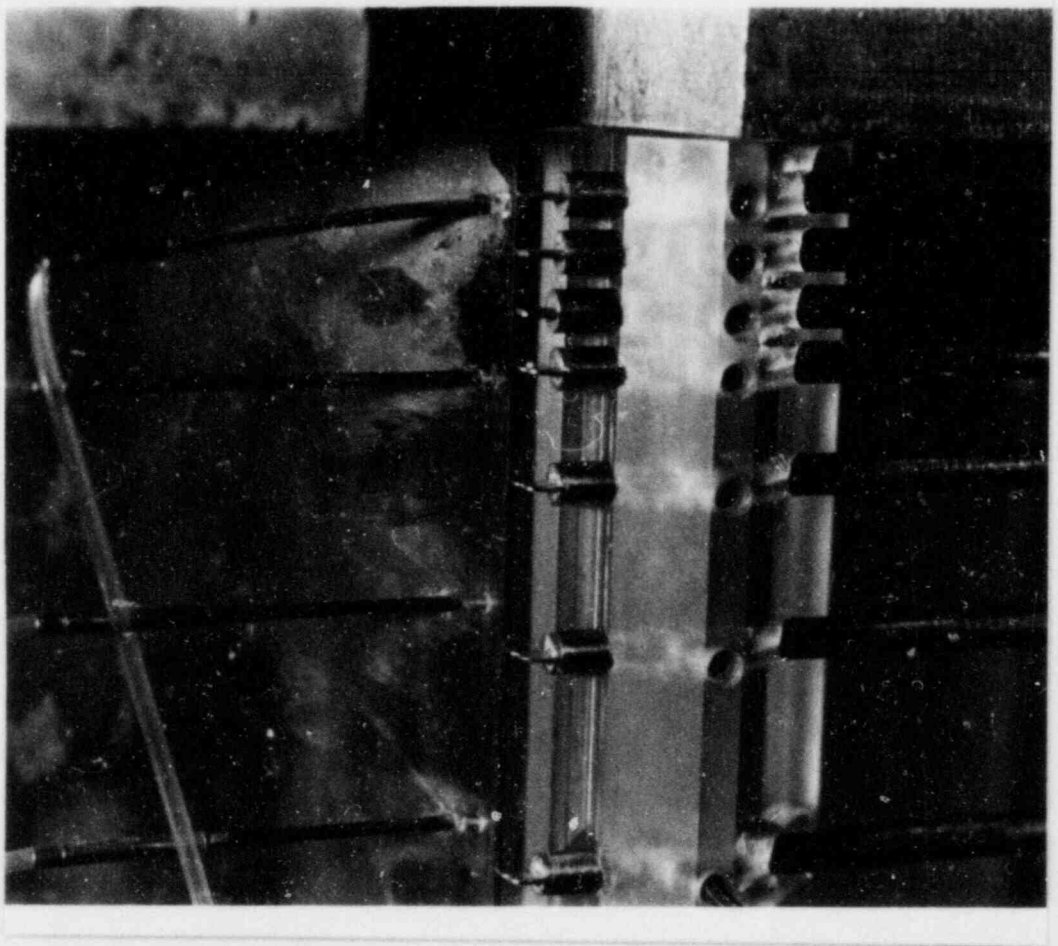

Figure 8. STAGNATION PROBES AT SEAM EXIT

to select individual probe outputs to be measured by the transducer. The voltage readings from the transducer were converted to pressure using the calibration data for the transducer. This calibration was performed using mercury manometers for the standard reference pressure.

The plenum pressure was the only variable in the quality-assured tests. Plenum pressure was measured using calibrated pressure gauges connected to the plenum at two locations. One gauge measured the pressure from the end of the plenum, while the second gauge was connected to the side of the plenum, at approximately mid-length. These two gauges always read within 0.5 psi of each other. The plenum pressure readings, corrected for elevation and averaged together, defined the downcomer-to-core differential pressure for these tests.

The flow rate to the model was measured using an orifice meter designed and installed in accordance with standard practice established by ASME (Reference 3). The orifice meter was fabricated from 2 inch diameter, schedule 40 pipe with flange taps. The orifice plate had a diameter of 1.551 inch (β=0.75), and an orifice coefficient (K-factor) in these tests of 0.61. A differential pressure transducer measured the orifice pressure drop.

All tests were conducted with cold water, in the range from 50°F to 60°F. Water temperature was measured in the supply tank using a dial-stem thermometer.

Table 1 provides a list of the test measurements, instruments, and estimates of the uncertainty in the measured and the reduced parameters.

TABLE 1

Test Measurement Uncertainties

Test Measurement	Instrument	Instrument Uncertainty	Uncertainty in Reduced Data
Inlet plenum pressure	gauge (2) (0 to 30 psig range)	0.5 psi	0.5 psi
Stagnation pressure	transducer (0 to 20 in. Hg range)	0.1 in. Hg	0.5% of velocity at 30 ft/s
Flowrate	transducer across orifice plate (0 to 20 in. Hg range)	0.1 in. Hg	5% of flowrate at 150 gpm*
Temperature	dial-stem thermometer (0 to 250°F range)	3°F	<0.1% of density at 60°F

* This uncertainty in flow rate also includes the combined uncertainty in the orifice discharge coefficient and other possible error sources.

3. FULL-SCALE MODEL TEST DATA

A series of Quality Assured tests were carried out in the full-scale model, measuring the leak flow velocity at the seam exit for three values of downcomer-to-core differential pressure. The nominal pressures selected for these tests ranged from 22.5 to 27.5 psid, covering the specified differential pressure of 25 psid and variations of ± 10% around that value. For the tests described in this section the model had a seam width varying between 0.015 inch and 0.017 inch over the height of the test section. In the region of the test section where the stagnation probes were situated the seam width was measured as a uniform 0.015 inch.

The tests were conducted following the procedures described in the test plan report (Reference 1). The basic procedure was to adjust the inlet flow rate to the model to achieve the target inlet plenum pressure. Then, with steady flow established the stagnation pressure from each of the seam exit probes was recorded. After a full set of probe readings for one flow condition, the flow rate was adjusted for a new inlet plenum pressure and the stagnation probe readings were again recorded. This process was repeated for each of the three inlet pressures values.

Following the tests the stagnation probe readings were converted to velocity according to the relationship in Eq. 2. The test results are shown in Figure 9. In that figure the velocity measured at each probe is plotted as a function of probe position relative to the bottom of the former plate with plenum pressure as a parameter. The size and elevation of the core hole are shown on the figure for reference.

The measured volumetric flow rate and the calculated Core Jet Velocity are also tabulated in Figure 9 at each of the test pressures. Core Jet Velocity is the ideal velocity which would be attained by a jet of water flowing through an orifice having a pressure drop equal to the tabulated plenum-to-core differential pressure.

$$V_j = \left(\frac{2 g_c \Delta P_c}{\rho} \right)^{1/2} \qquad (3)$$

where V_j = ideal jet velocity (ft/s)

ΔP_c = plenum-to-core differential pressure (lb_f/ft^2)

The data in Figure 9 show a peak seam flow velocity of about 35 ft/s at the probe located near the centerline elevation of the core hole (Probe 58). That peak velocity was measured for the test condition with the highest inlet plenum pressure (27.3 psid). At the specified pressure drop of 25 psid, the peak velocity at the seam exit was 34 ft/s. The peak velocity was still lower for the lowest pressure tested. These peak velocities are about 50% of the velocities achieved in the jet flow through the core barrel hole.

For all three test pressures the velocity profiles at the seam exit have the same characteristic form. The peak velocities occurred at the elevation of the core jet with lower seam flow velocities at elevations below the jet.

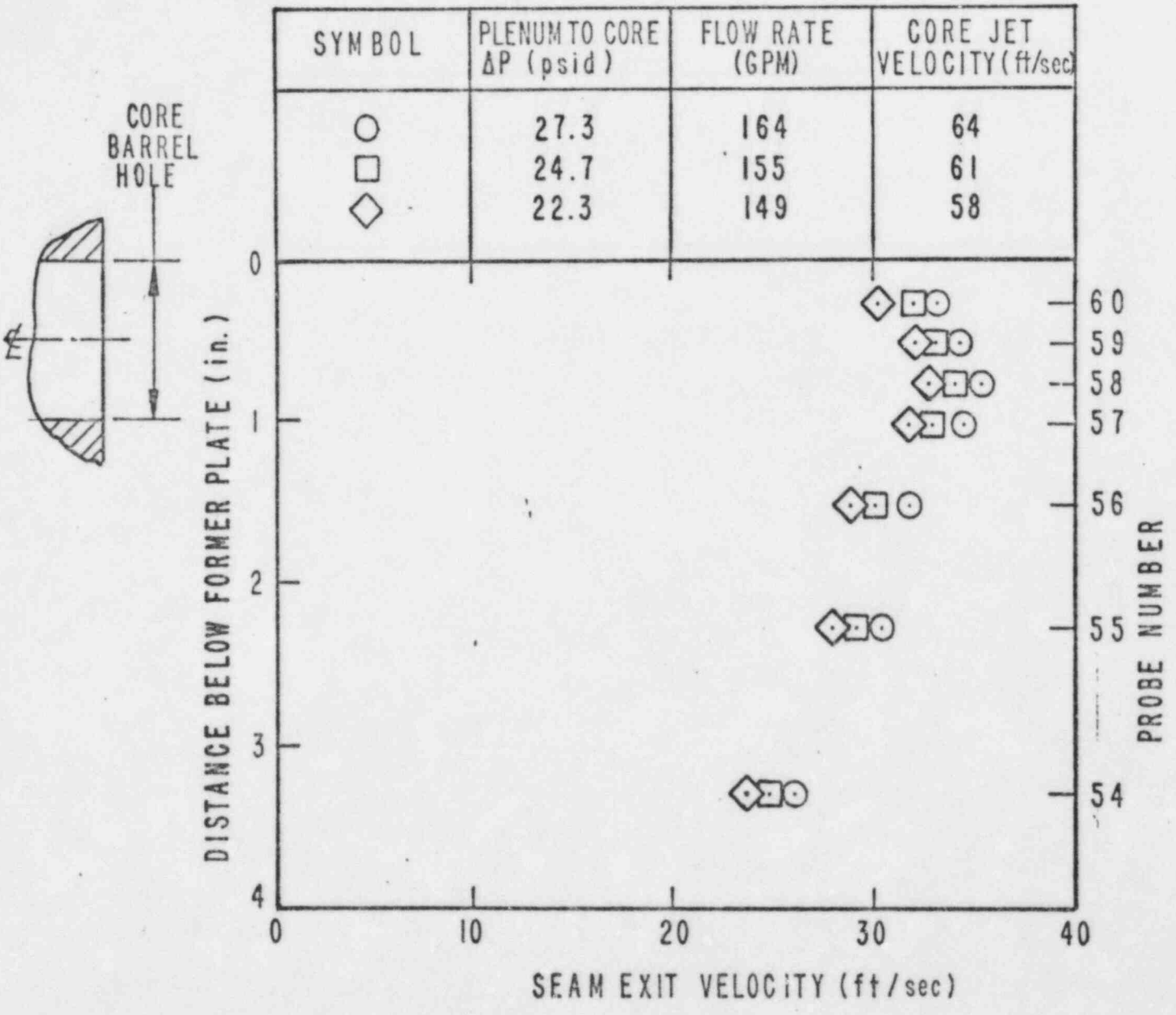

Figure 9. MEASURED SEAM LEAK FLOW VELOCITY

4 FLOW VISUALIZATION MODEL STUDIES

Brief flow visualization studies were performed to support the quality-assured data in the full scale model. The main purpose of these studies was to increase confidence in the identification and understanding of the flow phenomena, although some supportive data were also obtained. The work involved direct observation and manual interaction with the flow.

4.1 The Flow Visualization Model

A model of one sector (wedge) was constructed at full size, but reduced height. Figure 10 shows the model dimensions. The model stands 15 inches tall (approximately half of full height) and includes upper and lower horizontal plates, a vertical 90° wedge sector of the core shroud, and a vertical (flat) plate to simulate a section of the core barrel.

The model was submerged in cold water in a 300 gallon open trough having approximate dimensions 3 ft by 10 ft by 18 inches tall (liquid level). Baffling was inserted into the trough to reduce flow recirculation in order to suppress water surface turbulence and improve the flow visualization.

This model had two useful features which we exploited, namely accessibility and visibility. The model was small enough, and in an open tank, such that measurements could be made quickly and without questions of probe orientation or location. In this way simple traverses could be easily performed to survey the entire flow field. Spaces were large enough that a human hand could be moved through the flow to survey its main features. The model was constructed entirely of plastic to enable flow visualization (See Section 4.2).

Despite these useful features, this flow visualization work is for support information only. The data from this model are not quality assured and the model is not intended to be a precise replica.

4.2 Flow Observations

Figure 11 is a top view of the transparent model. Water is injected through a 1 inch pipe (1.05 inch I.D.) at the left of the photo. This pipe is installed at the bottom of the model for ease of flow visualization, and is correctly positioned relative to the base plate. (Gravity is irrelevant in a submerged flow.)

The Flow Between the Core Barrel and the Thermal Shroud

The flow is visualized by two skirts labeled A and B and located as in Figure 12. The individual black strips in these skirts deflect in the direction of the flow. Figure 11 shows that the water jet is narrow near the injection pipe and has a width about the size of the injection pipe. Near the corner the jet becomes a "corner flow" with flow toward the walls across the entire width except very near the side walls.

Similar flow observations throughout the region indicate the general flow pattern sketched in Figure 13. This artist's conception shows a compact jet entering at the bottom, turning upward in the corner, and turning back toward

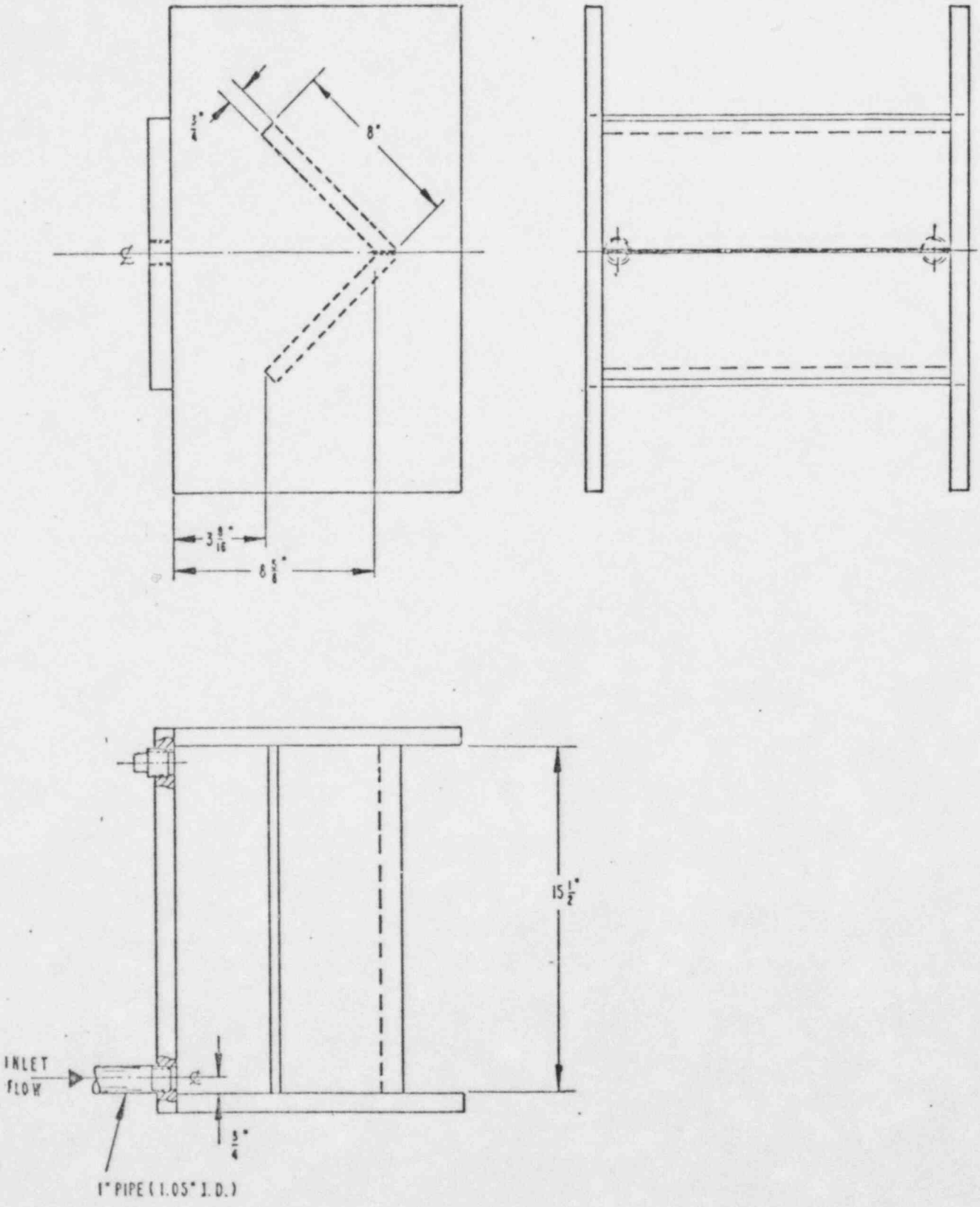

Figure 10. FLOW VISUALIZATION MODEL DIMENSIONS

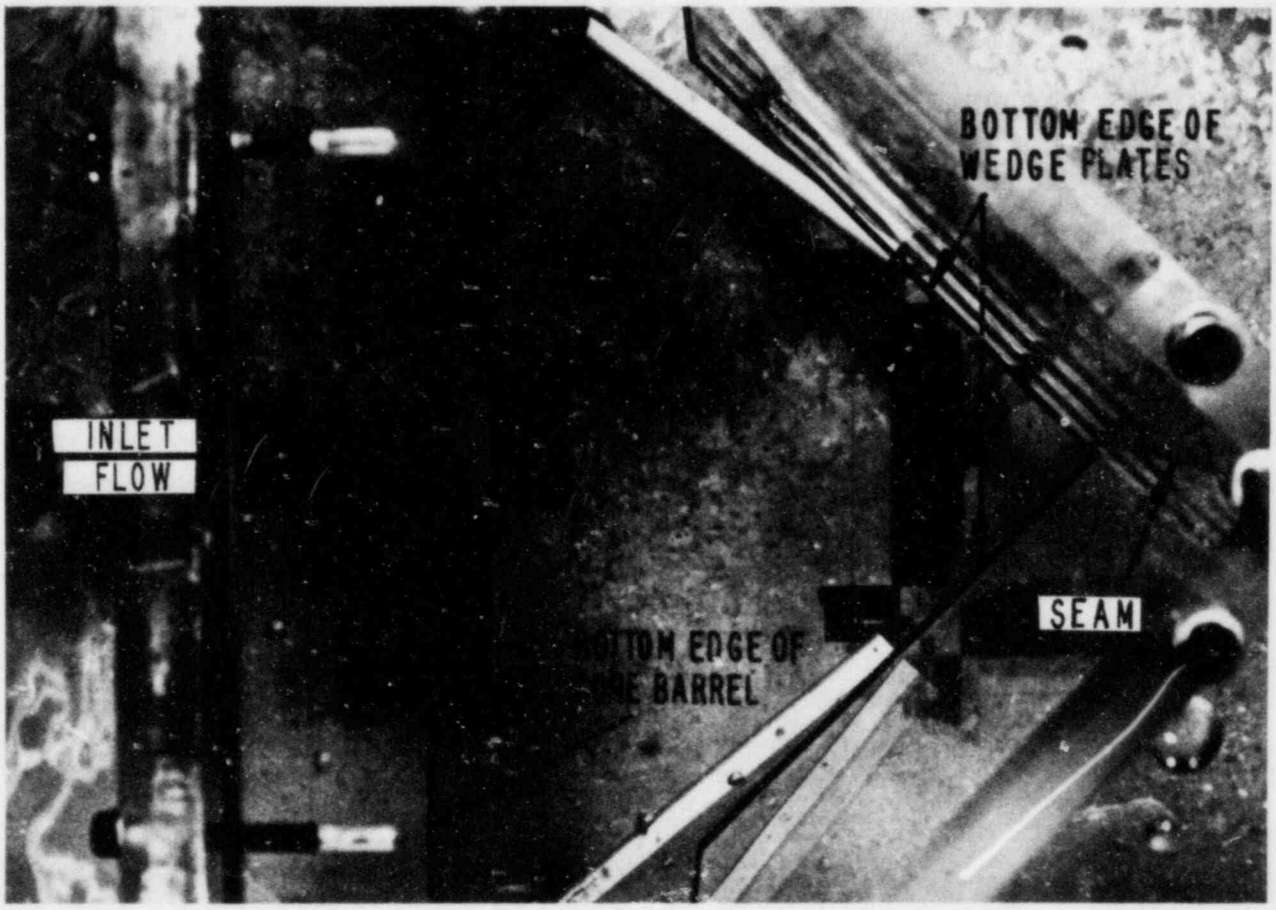

Figure 11. FLOW VISUALIZATION OF CORE JET

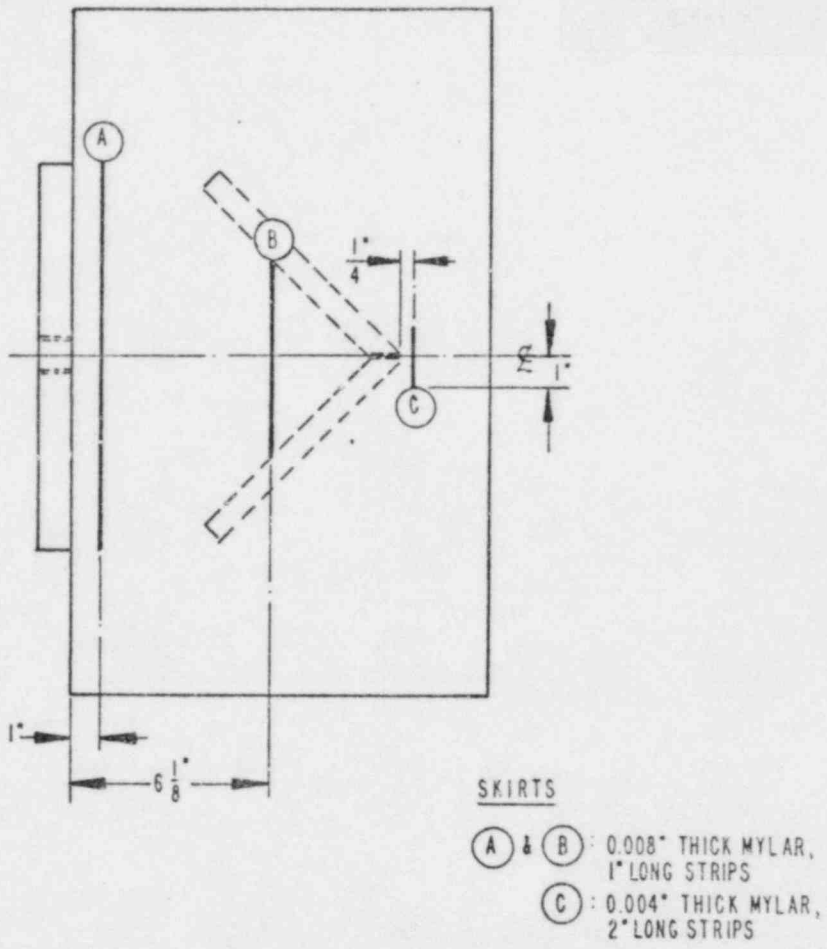

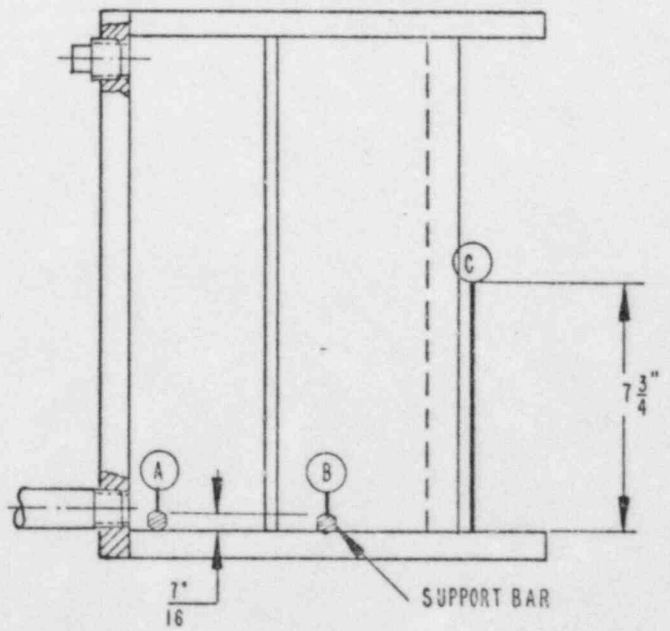

Figure 12. LOCATIONS OF FLOW VISUALIZATION SKIRTS

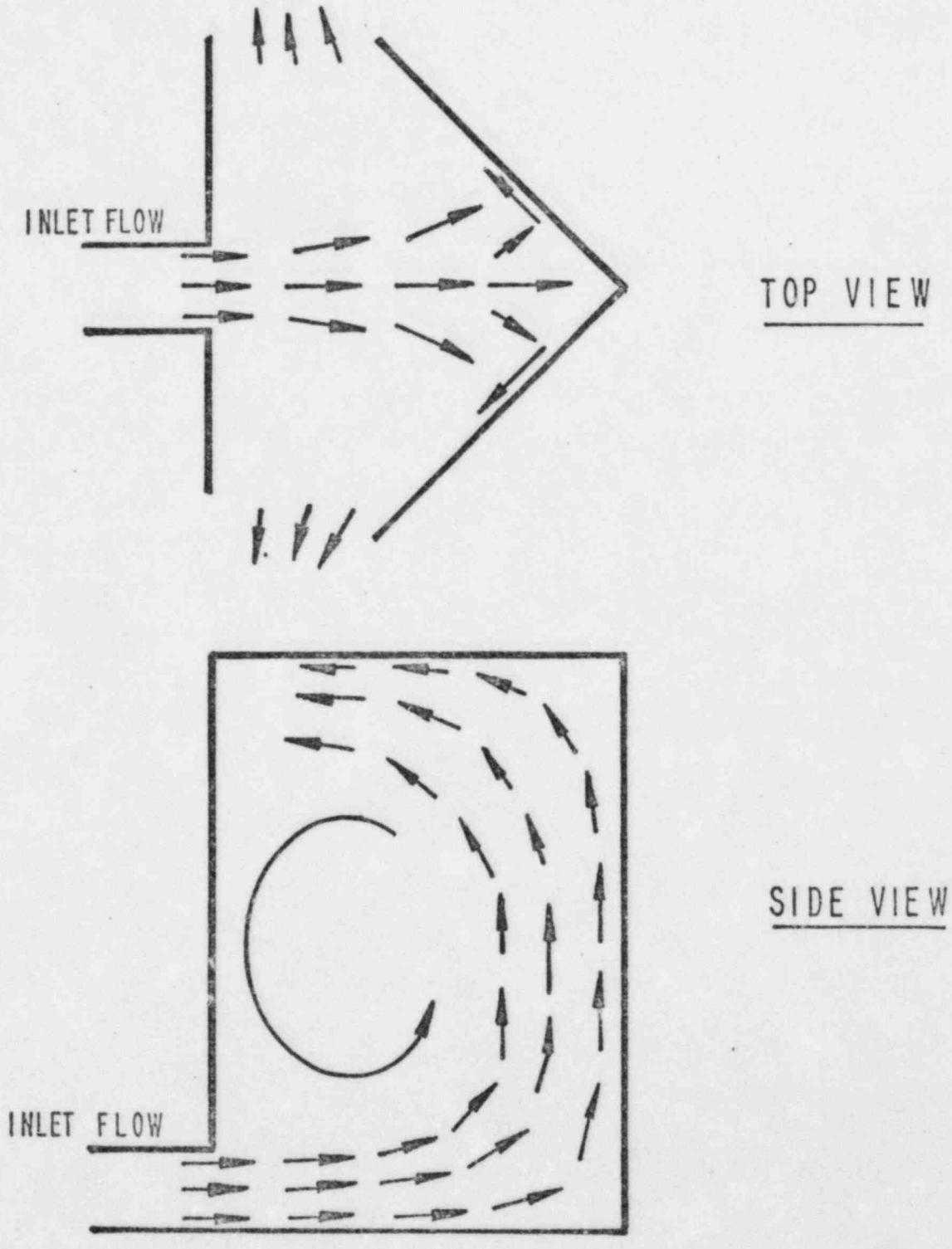

Figure 13. FLOW PATTERNS IN WEDGE REGION
(Artist's Rendition)

the core barrel at the top. There is considerable diffusion and turbulent mixing of this jet. In turn, this induces a major recirculating flow within the model.

The injected flow rate was varied over a factor of 5 range without observable change in either the overall flow pattern or the specific pattern seen in Figure 11.

The Flow through the Seam

Figure 12 shows the installation of a flow visualization skirt, labeled C, positioned outside the wedge. Skirts A and B and their support bars were removed during the tests of the flow through the slot, so as not to block the jet. The individual strips deflect according to whether there is a local flow through the seam. Figure 14 is a photograph taken at a 45° angle through the top of the model showing a typical flow pattern. The skirts deflect over a height h measured from the bottom; above this height no deflection is seen.

The height h of the seam exit flow depends on the flow rate and velocity of the injected jet. We performed a series of tests at various injection velocities and obtained the data given in Table 2. For comparison purposes, the range of injection velocities of the quality-assured data presented in Section 3 is 58 to 64 ft/s.

The last column of Table 2, labeled h "by finger probe" is a significant support measurement. An engineer reached around the top plate of the model and felt the flow issuing out of the slot with his index finger. The seam flow is very narrow, of order of the seam width which is 0.015 inches, and is so weak that the finger must be moved about to "find" the flow.

Comparison of the two methods used to measure h indicates that the skirts are slightly more sensitive than an index finger. It is difficult to imagine any substantial structure such as a rod being affected in the slightest by the very weak flow leaking through the seam.

In one series of measurements at an injection velocity of 54 ft/s (highest value) the flow visualization skirt was moved to the top of the model. The finger probe felt an outflow through the seam over about one inch of height and the skirts gave a deflection over 1.5 inches of height. The flow felt weaker (to the finger) at the top of the seam than at the bottom.

4.3 Stagnation Pressure Measurements

Additional supportive stagnation pressure measurements were made in the flow visualization model using hand-traversed probes. One probe was oriented to stagnate flow with direction toward the seam (horizontal) whereas the second probe stagnated flow in the vertical upward direction. The probes were both 1/8 inch in diameter and were located in the apex of the wedge at the inlet to the seam.

Figure 15 shows the stagnation pressure profiles in the flow visualization model at two inlet flow rates. The test data are displayed on two scales - stagnation pressure and the corresponding flow velocity - as a function of probe elevation above the bottom plate. The data clearly show a well defined corner

Figure 14. FLOW VISUALIZATION OF SEAM LEAKAGE

TABLE 2

FLOW VISUALIZATION TESTS
HEIGHT OF SEAM EXIT FLOW

Core Hole Flow (gpm)	Core Jet Velocity[1] (ft/s)	Span of Exit Flow[2] Skirts (in. ±¼")	Span of Exit Flow[2] Finger Probe (in. ±½")
41	15.2	3.5	too weak to feel
62	23	4.75	3.25
100	37.1	6.0	5.0
145	53.8	7.5	6.0
145	53.8	[1.5] Top[3]	[1.0] Top[3]

(1) The core jet velocity is calculated from the measured flow rate for a core hole diameter of 1.05 inch.

(2) The span of the exit flow is measured (inches) from the bottom plate of the model, with inlet jet at the bottom.

(3) The measurement in brackets is the span of the exit flow at the top of the model, with the inlet jet located at the bottom.

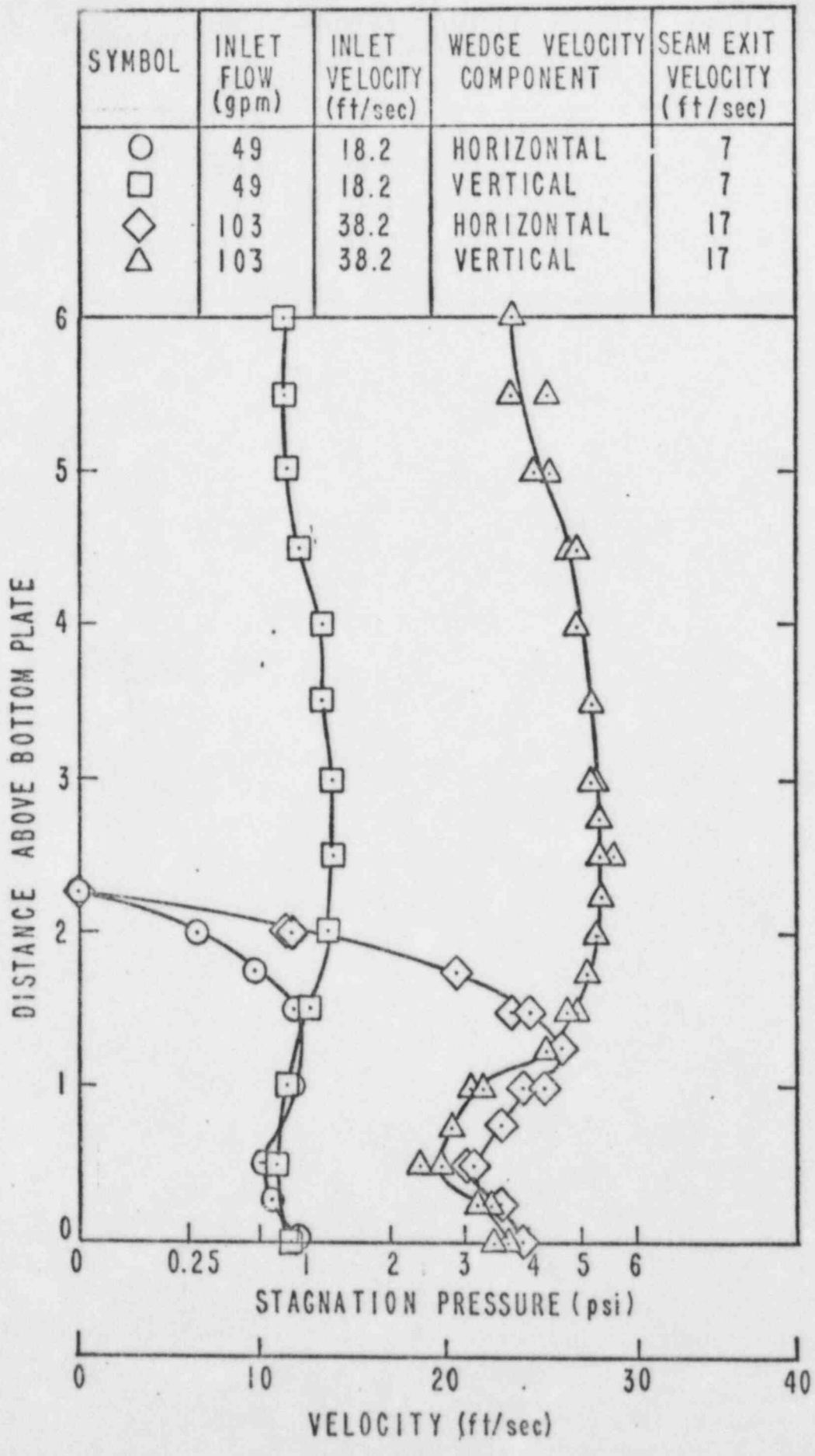

Figure 15. STAGNATION PRESSURE MEASUREMENTS IN WEDGE

flow close to the seam. The vertical extent of the horizontal component of the corner flow was measured to be only about 2 to 2.5 inches in height. The vertical upflow velocity (stagnation pressure) was also quite distinct, and was fairly uniform over the height of the model examined with the probes.

Compare the corner flow profile (Figure 15) with the measurements made with the flow skirts (Table 2). The height of the horizontal jet in the corner flow is less than half of the height of the seam flow. For example with a core inlet jet velocity about 37 ft/sec, Figure 15 gives a height of about 2.2 inches while the flow skirt gave a height of about 5 to 6 inches. The corner flow measurement is insensitive to core inlet velocity, as was the corner flow visualization, but the seam flow height is sensitive to core inlet velocity.

A single stagnation probe was also situated at the exit of the seam, 0.5 inch up from the bottom plate at the elevation of the inlet hole. The velocity of the flow leaking through the seam is shown in the tabulated data on Figure 15. For the two flow rates tested, the leak flow velocity was less than 50% of the inlet jet velocity.

These stagnation pressure measurements along with the flow visualization studies aid us in understanding the complex flow patterns in the region between the core barrel and the shroud assembly and provide confidence that we have located and measured the significant regions of leakage through the seam.

5 INTERPRETATION OF PHENOMENA

In an earlier letter report (Reference 4) we provided some qualitative descriptions of the phenomena acting to drive a small leakage flow through the seam in the shroud assembly. The recently completed experiments in the full-scale mockup, and the observations and measurements in the flow visualization model reinforce this early understanding of the flow behavior and provide quantitative data. In this section we offer new details to summarize and extend our earlier description of the flow phenomena.

Qualitative Description of Phenomena

Core Barrel Hole Jet - Driven by stagnation pressure in the downcomer, a water jet flows through the hole drilled in the core barrel. This jet contracts to some degree so that its diameter is smaller than the hole. Based on measured flow rate data in the full-scale model tests, the discharge coefficient, C_v, for the core barrel hole is estimated to be 0.83, implying a minimum jet diameter equal to 91% of the hole diameter ($D_j/D_H=\sqrt{C_v}$).

Free Jet - The jet enters the region between the core barrel and core shroud assembly. Bounded by the upper former plate, the jet remains relatively intact. However, it must travel a distance of order 10 times its diameter. As it does so, it entrains stagnant fluid and diffuses (spreads and slows down).

Recirculation Patterns - A complex three-dimensional flow is established in the space between the core barrel and the shroud assembly. Because the clearance gap between the shroud assembly and the core barrel is very large (flow area = 90 in^2) compared with the flow area of the jet (1.0 in^2) or the 0.015 inch wide crack (0.36 in^2), most of the jet flow leaves through this opening. That is, the jet turns and flows out the gap. There is also some inflow through the gap to feed the fluid entrainment by the jet. The sketch of flow patterns in Figure 13 is based on our observations in the flow visualization model.

While the flow patterns are quite complex, they have only a secondary impact on the jet. The measured jet stagnation pressures in the flow visualization model (Figure 15) show that the jet has retained approximately 60% of its inlet velocity by the time it reaches the apex of the "wedge".

Corner Flow - As the jet diffuses, there is little pressure recovery and the static pressure remains near zero. When the jet approaches the corner of the shroud assembly, it is deflected from horizontal to vertical. In turning the jet, an elevated static pressure is developed at the stagnation point in the corner of the shroud assembly, i.e. at the location of the seam inlet.

This corner flow occurs in a region of the order of one to three local jet diameters. That is, the corner region is about 3 inches on each side.

The flow continues vertically in the corner of the shroud assembly as a well defined jet, continuing to diffuse. As it approaches the former plate, the jet turns to the horizontal, toward the core barrel, again creating an increased static pressure in the corner of the shroud assembly.

Seam Flow - The static pressure developed by turning the jet drives a tiny leakage flow through the seam. The "width" (height) of this flow corresponds with the rise in static pressure due to the corner flow, but is somewhat greater due to diffusion within the seam. The velocity of the leakage flow is no more than the ideal velocity that could be achieved by converting the static pressure to dynamic head. In the flow visualization model tests the leakage flow velocity was only about 50% of the ideal velocity due to friction in the seam.

Coupling - The seam flow is much too small to influence the flow patterns elsewhere. That is, the inlet jet, the free jet, the recirculatory patterns, and the corner flow are insensitive to the size of the seam. The static pressure in the corner and the ideal velocity in the seam are the same whether the seam has width 0.010 inch, 0.015 inch, or 0.020 inch. The shape and width of the seam only affect friction in the seam. Based on results of preliminary tests described in Appendix A, the leakage flow velocity is proportional to the seam width b to the 1/2 power ($\sqrt{b}$).

Manual Calculations

For a seam velocity in the range 20 to 30 ft/sec, the Reynolds number and Fanning friction factors are tabulated below for a crack width of 0.015 inch.

	Cold (Model Test)	Hot (Reactor)
Re_b	3500-5000	18,000-27,000
flow	transitional	turbulent
f	0.02 - 0.05	0.025

Figure 16 tabulates and plots the velocity exiting the seam V_e, as a function of driving static pressure P_s, friction factor f, and crack width b.

Based on the measured stagnation pressures in the flow visualization model, we estimate a calculated leakage flow velocity of 16 to 20 ft/s leaving the seam. The experimental data in the flow visualization model show a velocity of approximately 17 ft/s. Thus, the measured behavior is consistent with simple theory.

SEAM EXIT VELOCITY VS. SEAM WIDTH

V_e = EXIT VELOCITY

V_i = IDEAL VELOCITY CORRESPONDING TO STAGNATION PRESSURE AT SEAM, IN ABSENCE OF FRICTION

$$V_i = \sqrt{\frac{2P_o}{\rho}}$$

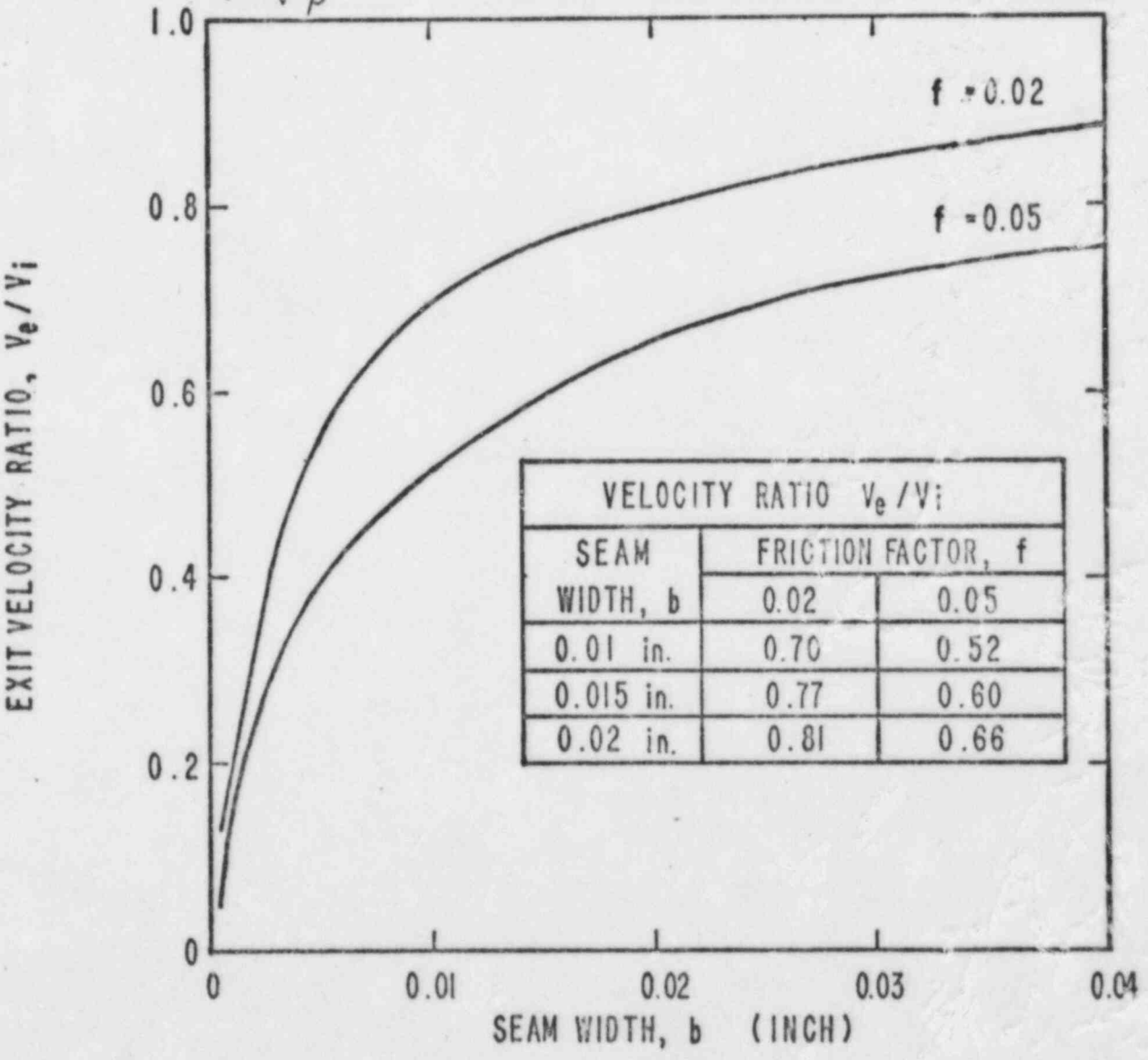

VELOCITY RATIO V_e/V_i		
SEAM WIDTH, b	FRICTION FACTOR, f	
	0.02	0.05
0.01 in.	0.70	0.52
0.015 in.	0.77	0.60
0.02 in.	0.81	0.66

Figure 16. SEAM EXIT VELOCITY VS. SEAM WIDTH

6 REFERENCES

1. Dolan, F.X., Rothe, P.H. and Sellew, S.S.; CORE JET TEST PROGRAM TEST PLAN AND PROCEDURE; Rev. 2, TM-952, Creare R&D Inc., Dec. 8, 1983.

2. Dean, R.C., Jr.; AERODYNAMIC MEASUREMENTS; Gas Turbine Laboratory, MIT, 1953.

3. Bean, H.S., ed.; FLUID METERS. THEIR THEORY AND APPLICATION; 6th ed., New York, NY: ASME, 1971.

4. Dolan, F.X. and Rothe, P.H.; Technical Memorandum to Frank Mello, Northeast Utility Service Co.; TM-950, Creare R&D Inc., Nov. 23, 1983.

APPENDIX A

Documentation of Preliminary Data

Preliminary tests conducted in the full-scale model provide additional data which support predicted trends and calculations of leakage flow velocity. This Appendix describes the results of two such preliminary tests which show the effects of seam width and downcomer-to-core differential pressure on seam leakage velocity. Because these tests were not fully quality-assured we have not incorporated the results in Section 3. However, it is our opinion that the data are correct and that the results are useful, and so we include them here for completeness.

Effect of Differential Pressure on Seam Exit Velocity

An early series of tests in the full-scale model covered the range of plenum-to-core differential pressures from 15 to 25 psid, compared with the quality-assured tests which covered a narrow range around 25 psid. For these early tests, the measured seam exit velocity showed a very clear trend with differential pressure. Table A-1 displays the data from these early tests having a seam width of 0.017 inch to 0.020 inch. In order to simplify the data tabulation, the leakage velocities measured at probes 57, 58, 59 and 60 are averaged together at each differential pressure ΔP_c. These probes cover the first 1 inch of seam height below the rib plate, where the maximum leakage velocities were measured. For the tests in Table A-1 the variation in velocity over this height was less than 1 ft/s. The column labeled "Normalized Velocity" compares the average seam velocity to the ideal core jet velocity as determined from Eq. 3. In these tests the leakage velocity was about 55% of the ideal core jet velocity and is proportional to $\sqrt{\Delta P_c}$ over the range of pressures tested.

Table A-1

Effect of Inlet Pressure on Seam Exit Velocity (1)

Inlet-to-Core Differential Pressure, ΔP_c (psid)	Calculated Core Inlet Jet Velocity, V_j (2) (ft/s)	Measured (3) Leakage Flow Velocity, V (ft/s)	Normalized Velocity V/V_j
14.7	46.7	25.8	0.55
19.5	53.8	28.8	0.54
24.4	60.2	33.3	0.55
24.5	60.3	33.8	0.56

(1) Data from tests with seam width variation from approximately 0.017 inch to 0.020.

(2) V_j is the calculated velocity of the inlet jet through core barrel hole, see Eq. 3.

(3) Tabulated velocity V is average of measurements from probes 57, 58, 59, 60.

Effect of Gap Width on Leakage Velocity

Figure 16 (Section 5) predicts a trend of increasing leakage flow velocity with increasing seam width b due to a reduction in friction pressure drop. The results from one early test confirm this basic trend. In that test the seam width was set at 0.02 inch, rather than the desired 0.015 inch. Tests were conducted in this configuration with inlet differential pressures of 22.3, 24.8 and 27.3 psid. The velocity measured with the stagnation pressure probe located at the centerline elevation of the inlet jet (Probe 59) is 10% to 12% higher in the tests with the 0.020 inch seam as compared to tests with the 0.015 inch seam at the same inlet pressures. This increase in velocity is consistent with the expected trend for the seam widths tested and for a Fanning friction factor f=0.05.

APPENDIX B

Velocity Diagrams from FLUENT Calculations

Introduction

Creare's proprietary computer-code FLUENT was used in early phases of this investigation to provide some insight into the overall flow patterns and magnitudes of velocities which might be expected in the experimental phase.

Examples of velocity vectors and profiles calculated using FLUENT are presented in this appendix as supplementary information. The flow patterns shown agree with our general assessment and descriptions of the phenomena in Section 4.2.

Physical Model

The physical model which was used in the calculations is a full-scale representation of the region bounded by the inner core barrel wall and the central wedge of the shroud, and by former plates on the top and bottom. Clearance gaps between the former plates and core barrel and between the shroud and core barrel were maintained at full-scale. The core barrel was simulated with a flat plate to simplify the configuration of the finite-element mesh. The hole through the core barrel was modeled as a square opening having an area equivalent to the area of a circular opening with a diameter of 1 1/8 inch. Fluid properties for water at prototype reactor operating conditions were assumed, and a core barrel hole pressure drop of 20.6 psid was used in the calculations.

Velocity Diagram

Figures B-1 through B-6 display calculated velocity vectors and profiles in two views of the core barrel/fuel shroud geometry. Velocity direction at a location is indicated by the arrow alignment and magnitude is scaled from the vector length relative to the longest vector in the displayed field. The maximum velocity is given in m/sec in the lower left of each figure.

The three velocity profile diagrams provide additional details of the local patterns and changes in distribution of a single component of velocity in a plane. Again, the velocity scale factors are given in the lower left figure label.

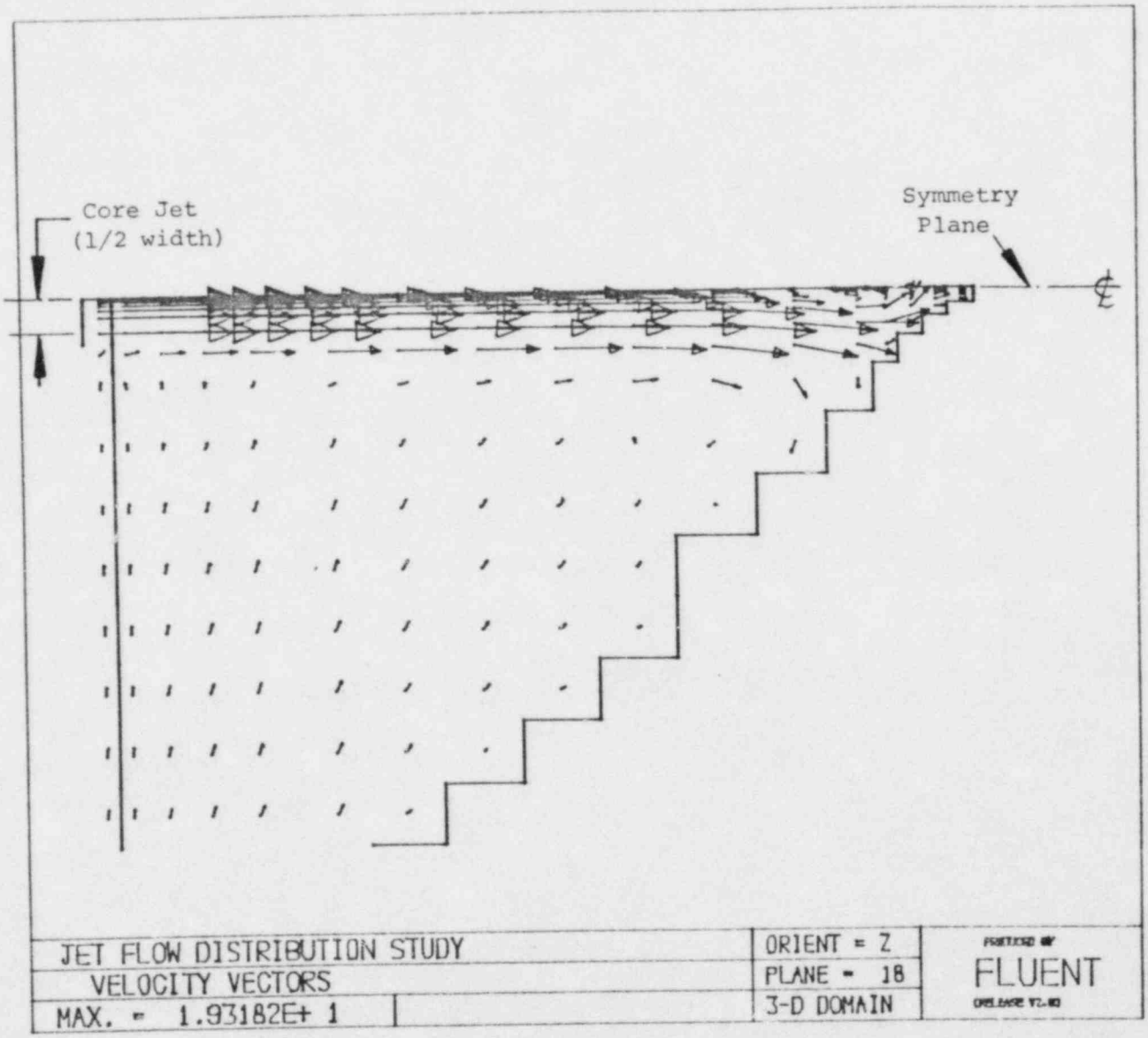

Figure B-1. VELOCITY VECTOR DIAGRAM HORIZONTAL PLANE THROUGH CENTERLINE ELEVATION OF CORE JET

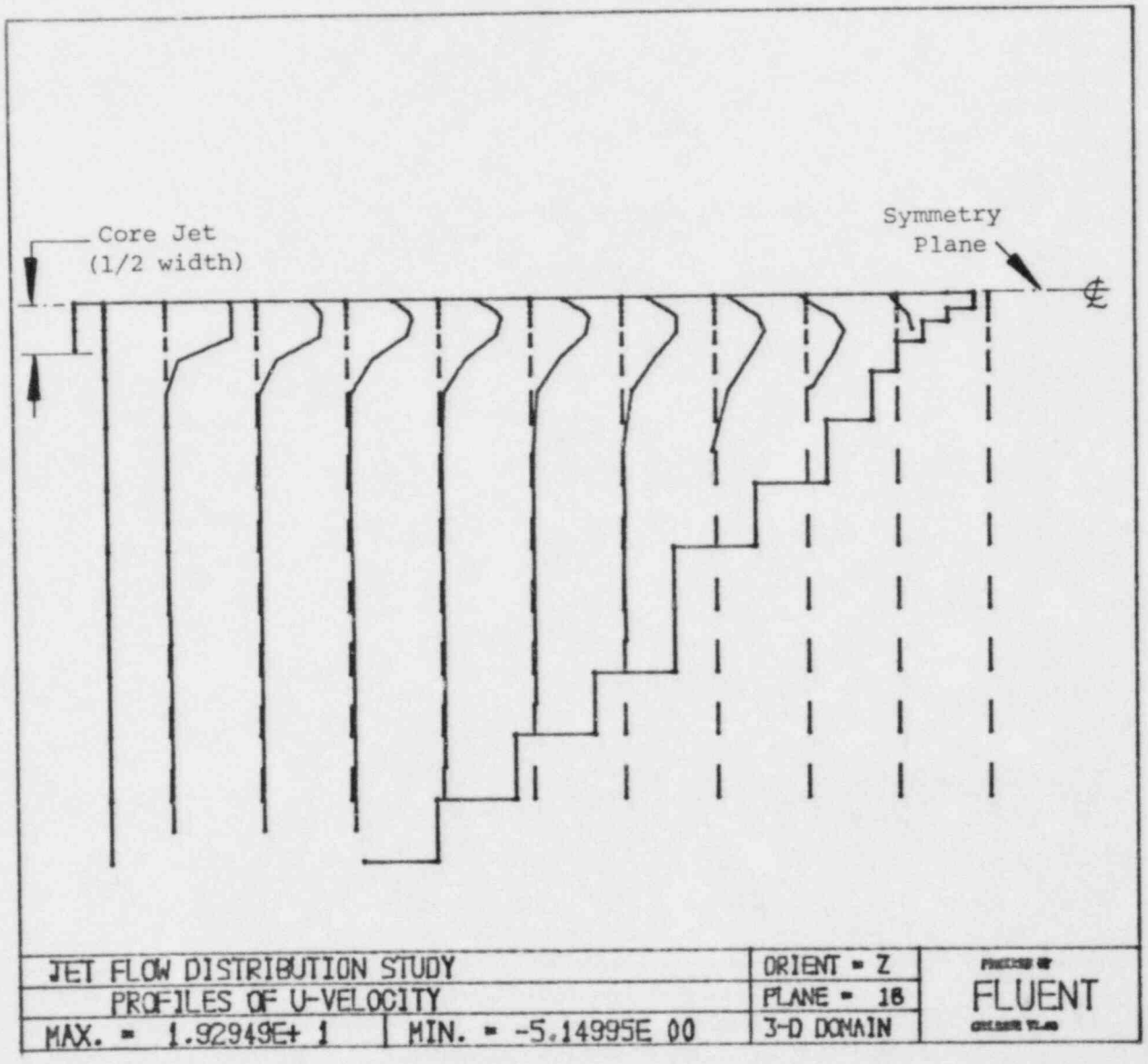

Figure B-2. VELOCITY PROFILE DIAGRAM U-COMPONENT IN HORIZONTAL PLANE THROUGH CENTERLINE ELEVATION OF CORE JET

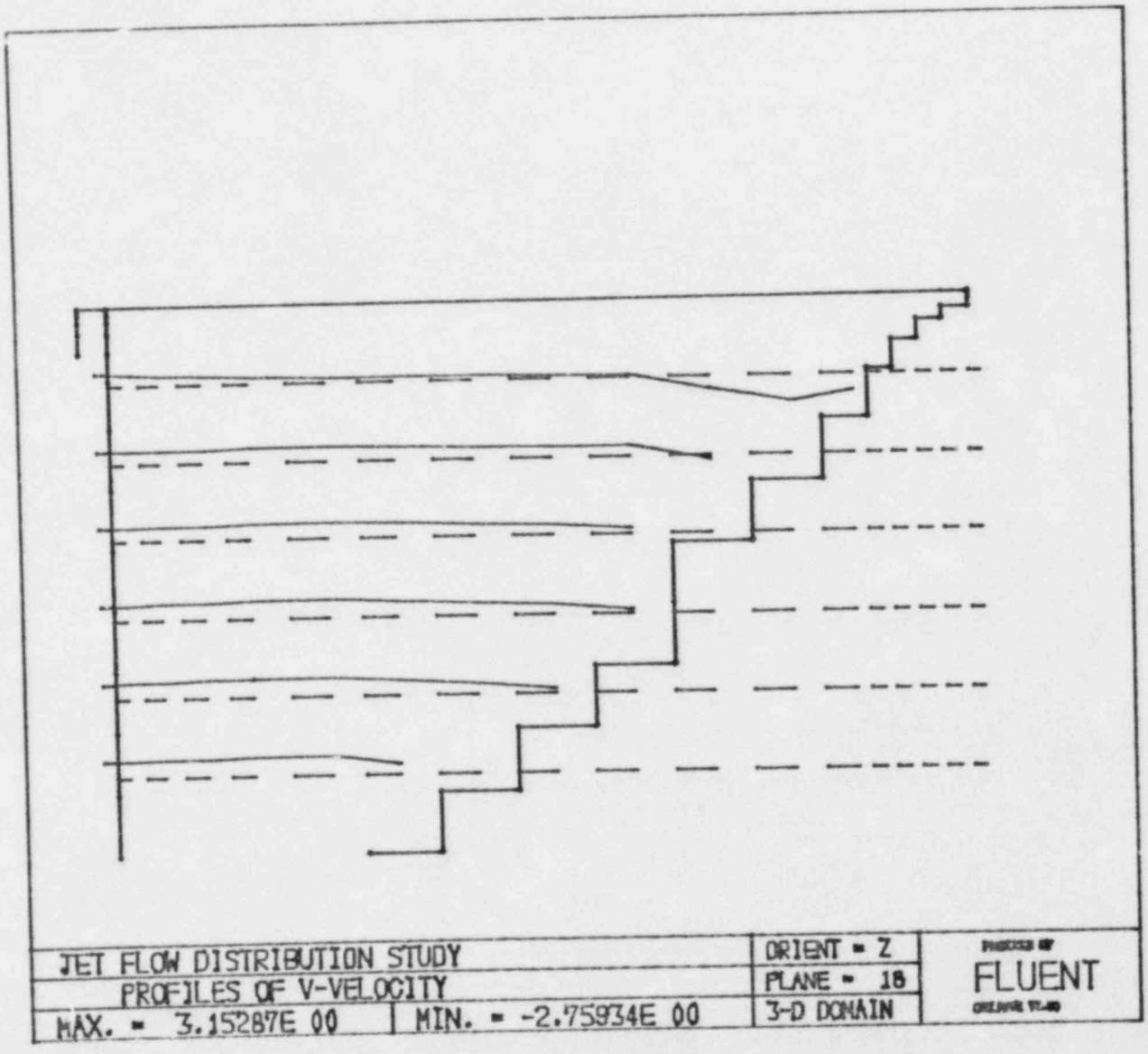

Figure B-3. VELOCITY PROFILE DIAGRAM V-COMPONENT IN HORIZONTAL PLANE THROUGH CENTERLINE ELEVATION OF CORE JET

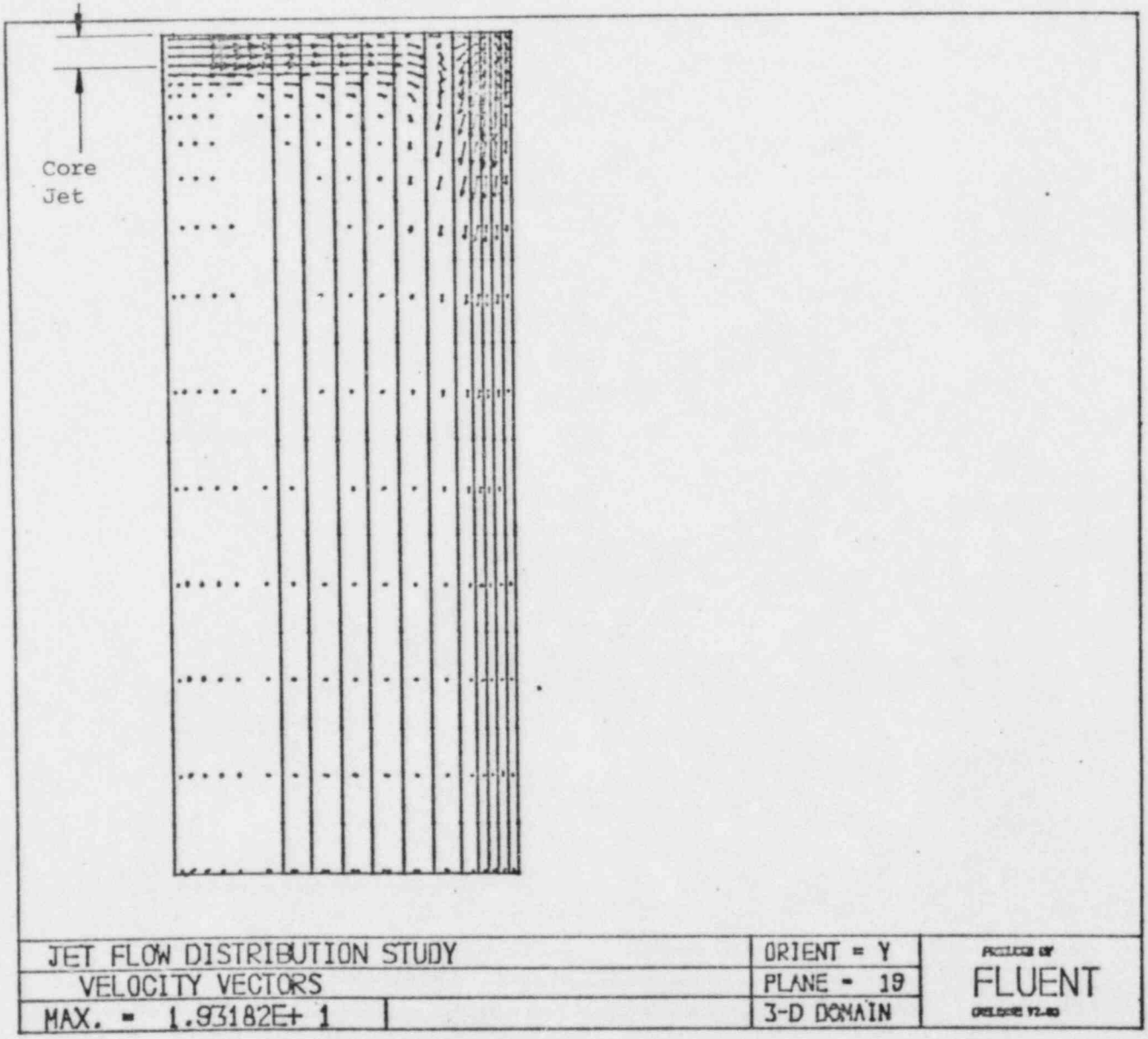

Figure B-4. VELOCITY VECTOR DIAGRAM VERTICAL PLANE THROUGH CENTERLINE OF CORE JET

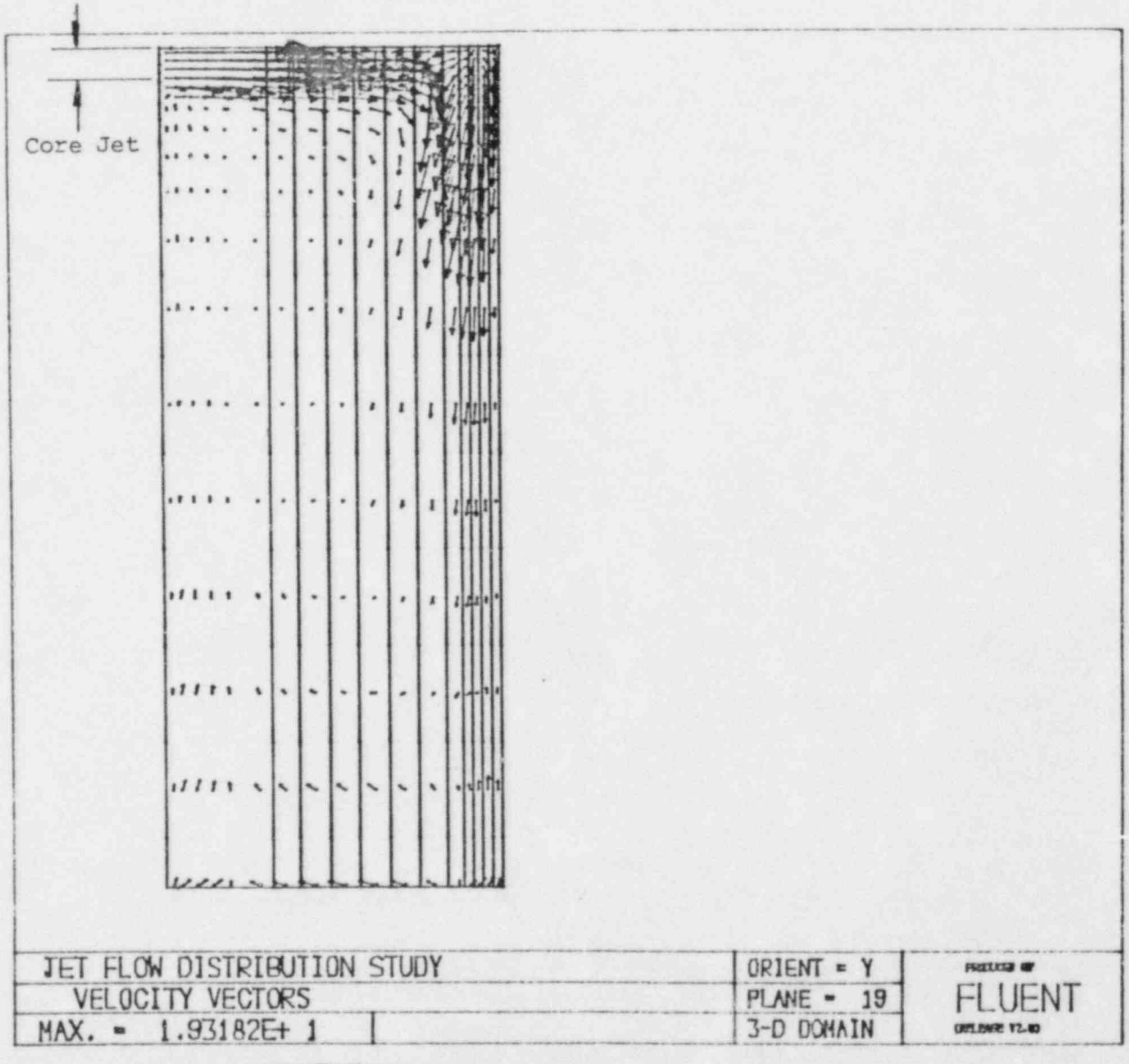

Figure B-5. VELOCITY VECTOR DIAGRAM (SAME AS FIGURE B-4 WITH MAGNIFIED VECTOR LENGTH)

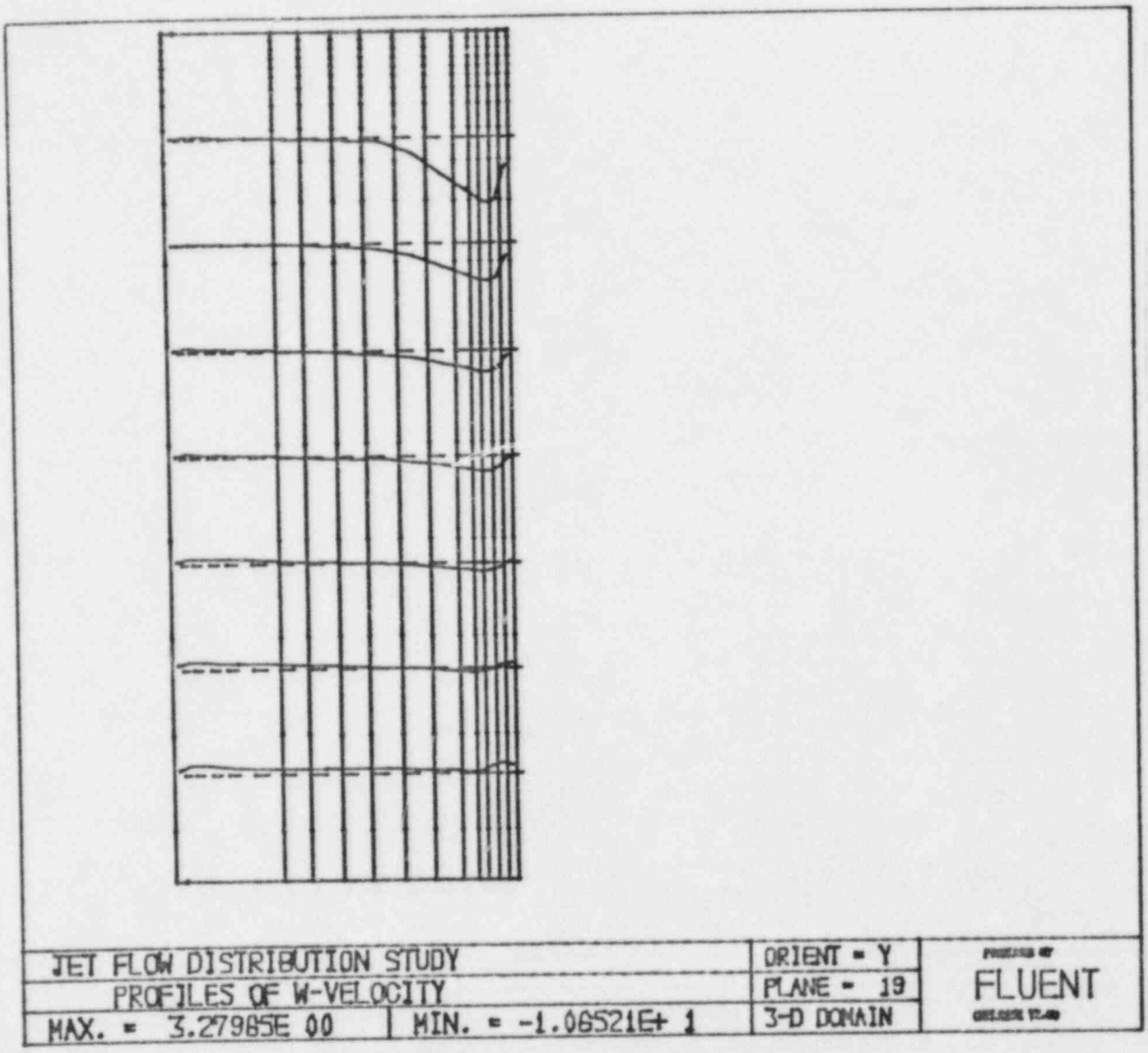

Figure B-6. VELOCITY PROFILE DIAGRAM W-COMPONENT IN VERTICAL PLANE THROUGH CENTERLINE OF CORE JET

A.2 Effects of Core Shroud Baffle Jetting on Fuel

GENERAL DESCRIPTION OF EVALUATIONS

Fluid elastic fuel rod response to baffle jet conditions is determined by a concatenation of data obtained from mechanical testing and analysis. The type of data/analyses required to judge rod stability includes the determination of fuel rod mechanical properties and determination of the effective baffle jet momentum flux. These calculations and tests lead to the establishment of an allowable momentum flux criteria.

In order to analyze fuel rod motion, the fuel rod mechanical properties must be determined. The properties necessary to characterize fuel rod motion include fuel rod damping, stiffness, mass, and support conditions (BOL and EOL). These parameters are used in the analytical evaluation of the fuel rod natural frequencies and mode shapes. The analytical models are then used in the effective momentum flux calculation.

The baffle jet effective momentum flux profile, V^2h, is determined analytically using the velocity profile obtained from a hydraulic resistance model and verified by full scale hydraulic test data presented in Section 1. The effective momentum flux is calculated by normalizing the absolute momentum flux through the core shroud gap to the fuel rod mode shapes. The calculation is performed using the following equation.

$$V^2h_{eff} = \frac{\int_0^L V^2h(z)\emptyset^2(z)dz}{\int_0^L \emptyset^2(z)dz} \qquad (1)$$

where $\emptyset(z)$ - the normalized mode shape

The fuel rod motion resulting from an applied hydraulic flux excitation was determined experimentally. During hydraulic testing, rod motions were closely monitored to determine the instability points. Once established, the effective momentum flux inducing the instability was used to develop the stability criteria.

The stability criteria were based on Comov's stability equation which relates the fuel rod mechanical properties to momentum flux. The equation is given below.

$$V^2h = \frac{B^2Fn^2D\delta M_o}{\rho} \qquad (2)$$

where

- B - The Fuel Assembly Constant
- F_n - Fuel Rod n^{th} Mode Frequency of Vibration
- D - Fuel Rod Outside Diameter
- δ - Fuel Rod Log Decrement Damping
- M_o - Fuel Rod Mass Per Length
- ρ - Fluid Density

The allowable momentum flux was determined by retrofitting the test data using equation 2 to establish the constant beta, bound by a square distribution at a 95% confidence level extrapolated to zero failures (instabilities). Once established the measured fuel rod parameters are used in conjunction with beta to determine the allowable v^2h.

EVALUATION

The Millstone Unit No. 2 plant specific analysis was performed utilizing the core shroud seam exit velocity profile determined experimentally as discussed in Section 1. Since the velocities were measured at room temperature, they were converted to the velocities at operating temperature by multiplying the original values by a factor of 1.203 to account for the density effect. Furthermore, the velocity profile was modified to fit the finite-element fuel rod model. The modified velocity profile was slightly more conservative and thus, would yield more conservative results. Figure 1 shows the original velocity profile determined experimentally and the modified velocity profile used in the analysis.

The values of momentum flux were calculated for the first nine fuel rod vibration modes. Since the effective V^2h values are less than the allowable V^2h values for all the first nine fuel rod vibration modes, it is concluded that the core shroud seam exit jet flow will not cause fuel rod instability.